

Binding in alkali and alkaline-earth tetrahydroborates: Special position of magnesium tetrahydroborate

Zbigniew Łodziana*

*Hydrogen & Energy, EMPA, Swiss Federal Laboratories for Materials Testing and Research,
Überlandstraße 129, CH-8600 Dübendorf, Switzerland
and Institute of Nuclear Physics, Polish Academy of Sciences, ulica Radzikowskiego 152, PL-31-342 Kraków, Poland*

Michiel J. van Setten

*Institute of Nanotechnology, Karlsruhe Institute of Technology, P.O. Box 3640, D-76021 Karlsruhe, Germany
(Received 1 October 2009; revised manuscript received 10 December 2009; published 29 January 2010)*

Compounds of light elements and hydrogen are currently extensively studied due to their potential application in the field of hydrogen or energy storage. A number of new interesting tetrahydroborates that are especially promising due to their very high gravimetric hydrogen content were recently reported. However, the determination and understanding of their complex crystalline structures has created considerable debate. Metal tetrahydroborates, in general, form a large variety of structures ranging from simple for NaBH_4 to very complex for $\text{Mg}(\text{BH}_4)_2$. Despite the extensive discussion in the literature no clear explanation has been offered for this variety so far. In this paper we analyze the structural and electronic properties of a broad range of metal tetrahydroborates and reveal the factors that determine their structure: ionic bonding, the orientation of the BH_4 groups, and the coordination number of the metal cation. We show, in a simple way, that the charge transfer in the metal tetrahydroborates rationally explains the structural diversity of these compounds. Being ionic systems, the metal tetrahydroborates fall into the classification of Linus Pauling. By using the ionic radius for the BH_4 group as determined in this paper, this allows for structural predictions for new and mixed compounds.

DOI: [10.1103/PhysRevB.81.024117](https://doi.org/10.1103/PhysRevB.81.024117)

PACS number(s): 61.50.Lt, 65.40.-b, 71.20.Nr

I. INTRODUCTION

The metal tetrahydroborates, also called tetrahydroborates, borohydrides or, in short, boranates, are compounds containing metal cations and BH_4 groups. They have been shown to form with alkali and alkaline-earth elements, various transition metals, and with aluminum.^{1–14} In general, the number of BH_4 groups per metal atom reflects the valency of the cation. Recently, the tetrahydroborates have been studied intensively because of their high gravimetric hydrogen content, which makes them potential hydrogen storage materials.¹⁵

In the simplest picture, the tetrahydroborates can be thought of as ionic solids with metal cations and BH_4^- anions that are semicovalently bound molecular units. The valence electrons from the metal are transferred to the BH_4 groups which then have a sufficient number of electrons to fill an eight-electron closed-shell configuration. When this simple picture is used to model the enthalpy of formation using a Born-Haber cycle, a very reasonable agreement with known experimental values for the alkali and alkaline-earth tetrahydroborates can be found.^{16,17}

The crystal structure complexity of the tetrahydroborates increases with increasing valency of metal atoms. In general, structural complexity is attributed to an enhanced cation-hydrogen interaction. Other factors contributing to the complexity could be related to the increased number of anions per cation and the decrease in the cations' average size. In fact, for monovalent metals the agreement between experimental and theoretical data describing the low-temperature structural properties is excellent.^{18,19} For the

high-temperature phase of LiBH_4 , however, some discrepancies in understanding structural properties still exist.^{20,21}

The, only recently, determined crystal structures of the tetrahydroborates of magnesium and calcium show that the simple ionic picture might be too simple to predict the full details of their crystal structures. In the case of magnesium, a low- and a high-temperature crystal structure have been determined experimentally, both showing a high complexity.^{22–24} Additionally, high-pressure studies indicate the existence of other phases.²⁵ Besides these, two other crystal structures have been predicted by density-functional theory (DFT) studies that have a lower total energy than the experimentally determined structures.^{26,27} Even more structures have been predicted by DFT, all of which lay close in total energy to the experimental and more stable DFT structures.^{17,26,28–31} Such a large diversity of structures and discrepancy between theoretical and experimental results is not common for this type of materials.

In the case of calcium tetrahydroborate, three polymorphs have been found.^{32–39} The α phase transforms into the β phase around 130–170 °C.^{40–43} The γ phase only forms under specific conditions.^{35,36,44} In all cases, the calcium cation is coordinated by six BH_4 groups, two more than in the magnesium tetrahydroborate structures. For this compound and also for $\text{Be}(\text{BH}_4)_2$ there is a reasonable agreement between experimental and theoretical structural data.

At ambient conditions, the tetrahydroborate of aluminum $\text{Al}(\text{BH}_4)_3$ is a liquid. However, at low temperatures two distinct phases of this compound were identified, both possessing a complex crystalline symmetry.^{45,46} In the two solid phases and in the liquid phase, the aluminum cation is coordinated by three BH_4 groups and the structure is bonded via weak dispersive interactions.

TABLE I. The Bader charges (in electrons) on the atoms and the local structural parameters for the metal tetrahydroborates considered in the present work. Repeated numbers span the range of charges observed for inequivalent hydrogen ions. CN stands for coordination number for the metal cation and $d(M-B)$ is the average distance between metal cation and the nearest boron atoms in Angstroms.

System	Cation	B	H	CN	$d(M-B)$
LiBH ₄	+0.89	+1.62	-0.62 -0.64	4	2.50
NaBH ₄	+0.89	+1.62	-0.63	6	3.00
KBH ₄	+0.85	+1.63	-0.62	6	3.34
Be(BH ₄) ₂	+1.66	+1.62	-0.55 -0.67	3	1.89
Mg(BH ₄) ₂ ^a	+1.67	+1.60	-0.60 -0.62	4	2.40
Ca(BH ₄) ₂ ^b	+1.58	+1.60	-0.58 -0.60	6	2.90
Al(BH ₄) ₃	+2.29	+1.54	-0.50 -0.64	3	2.14

^a*F*222, this phase is considered as a representative for Mg(BH₄)₂. Other structures of this compound have the same coordination number and bidentate BH₄ orientation.

^b*P*4₂/*m*.

In this paper, we reveal the physical principles behind the variety of complex crystal structures seen in the tetrahydroborates. We study the interaction between the alkali elements Li, Na, and K, the alkaline-earth elements Be, Mg, Ca, and Al, and BH₄ groups using first-principles DFT calculations and analytic models for electrostatic interaction. We show that metal tetrahydroborates, as strongly ionic systems, obey the simple rules for atomic coordination proposed by L. Pauling for that class of compounds. Additional structural complication is present in tetrahydroborates due to tetrahedral symmetry of BH₄ group. From our studies, we explain the local geometries that occur in the known crystalline structures of the metal tetrahydroborates and link these to the details seen in the electronic structures of the solids. We show that the complicated structure of Mg(BH₄)₂ results from a combination of electronic and electrostatic effects.

II. CALCULATIONS AND MODELS

A. Computational details

All DFT calculations are performed applying the generalized gradient approximation for the exchange-correlation functional.⁴⁷ We used a plane-wave basis set and the projector-augmented wave method,^{48,49} as implemented in the Vienna *ab initio* simulation package VASP,⁵⁰⁻⁵³ and applied nonlinear core corrections.⁵⁴

The calculations on the clusters are performed using supercells. All are cubic with sides of at least 18 Å. These large cells are required to obtain the total energies converged within 0.01 eV. The reciprocal space is sampled by the Γ point only in this case.

The calculations of the solids are performed using \mathbf{k} -point samplings such that in all cases the total energy is converged within 1 meV/f.u. The Bader charge analysis was performed using a Gaussian smearing with a width of 0.05 eV and the grid for the charge density with spacing of 0.04 Å or denser. The calculations of the densities of states are performed using the tetrahedron method,⁵⁵ except for those compounds that have a large unit cell. In those cases, Mg(BH₄)₂ and

Be(BH₄)₂, a Gaussian smearing with a width of 0.1 eV is used.

B. Crystal structure of the solids

We start by studying in detail the local geometries as they occur in the solid-state crystals, adopting the following nomenclature. Under monodentate, bidentate, or tridentate orientation we understand the orientation of a BH₄ group with respect to a metal ion where one, two, or three hydrogen atoms are pointing toward the metal atom. Talking about the coordination number of a metal atom we always count the number of the nearest BH₄ groups.

The calculations for the solid phases were performed on the crystal structures of Be(BH₄)₂ reported in Ref. 56, those of Mg(BH₄)₂ as reported in Refs. 27 and 28, that of Ca(BH₄)₂ as in Ref. 33, LiBH₄ as in Ref. 20, NaBH₄ and KBH₄ as in Ref. 18, and Al(BH₄)₃ as in Refs. 45 and 46. All structures were optimized with respect to the lattice parameters and internal atomic positions in the appropriate crystallographic symmetry. The structural details of the crystals can be found in Tables S1–S3 of the supporting information.⁷³

An analysis of the atomic coordination and mutual orientation of the metal atoms and molecular groups provides an insight into local properties and the interaction between the atoms of all structures considered here. For lithium tetrahydroborate, the orientation of the BH₄ groups with respect to the tetrahedrally coordinated Li cation can be perceived as mixed bidentate and tridentate. For NaBH₄ and KBH₄, these groups are oriented in the bidentate configuration in an octahedral coordination around the central metal cation and their separation from the cation is significantly larger than in LiBH₄, see Table I. For compounds with divalent cations, the orientation of the BH₄ groups with respect to the metal cation also varies: in Be(BH₄)₂ and Mg(BH₄)₂ it is bidentate with Be coordinated by three and Mg by four BH₄ groups. In Be(BH₄)₂, the Be-B separation is the smallest cation-cluster separation of all compounds considered here (see Table I). The Ca cation is surrounded by six BH₄ groups, which are in mixed bidentate and tridentate orientations. In aluminum tet-

rahydroborate, the BH_4 groups are in bidentate orientation with respect to the central Al cation with a coordination number of three. In this system, the crystalline structure is built from stoichiometric $\text{Al}(\text{BH}_4)_3$ molecular units.

To sum up, the coordination number of the cations ranges from three to six and the orientation of the BH_4 groups with respect to the metal cations varies between bidentate and tridentate. A monodentate orientation is not observed in any of the compounds considered here. We will discuss these differences and their origin in more details in the following parts of this paper.

The nature of the bond between metal atoms and BH_4 groups can be examined by analysis of atomic charges in the system.^{57,58} The Bader charges, see Table I, on the atoms show a trend of decreasing ionicity with increasing valency of the cation; the average charge on the BH_4 groups varies between $\sim 0.88e$ for monovalent cations through $\sim 0.82e$ for divalent and $\sim 0.77e$ for $\text{Al}(\text{BH}_4)_3$. A similar trend among atoms from the same column of the periodic table does not exist. Moreover, there is no simple relation between metal-boron distance and the charge transfer.

According to the Bader analysis, all compounds are strongly ionic. Within the BH_4 groups, the electronic charge is also not distributed homogeneously. The majority of the electronic charge is located on the hydrogen atoms, which is in accordance with the Pauling electronegativity of hydrogen and boron (2.2 for H and 2.0 for B). In the following sections we present studies which clarify the relationships between the coordination number of the metal cation, the orientation of the BH_4 groups with respect to a central metal cation, and the dimensions of the cation.

C. Interaction of a single BH_4 group with a cation

To get a clear picture of the first-order effects of the interaction between the cations and a BH_4 group, we focus first on the interaction of a single group with the series of cations. The systems are modeled by fixing the BH_4 group and rotating the cation around it for a series of metal-boron distances. The rotation is chosen in such a way that the cations are initially in bidentate orientation at 0° , then reach the tridentate orientation at 54.74° , a monodentate orientation at 125.26° , and come back to the second bidentate orientation at 180° . Using DFT, we calculate the total-energy landscape of the system as a function of the rotation angle and the cation-boron distance. In all calculations, neutral atoms are placed in the supercell.

It is evident from Fig. 1 that in all cases the tridentate orientation of BH_4 with respect to the central metal atom is the global minimum of the total energy. The bidentate orientation is slightly less favorable (~ 0.2 – 0.4 eV), with the equilibrium distance being 0.2 Å larger than the optimal distance in the tridentate orientation, see Table II. The monodentate orientation is in all cases significantly less favorable (>1.0 eV) at an optimal distance of about 1 Å larger than the optimal distance in the tridentate orientation. The energy difference between tridentate and bidentate orientations varies only slightly between the different cations while the

difference in energy between the tridentate and the monodentate orientations varies by an order of magnitude more.

The atomic radii of the metal cations correlate with the equilibrium metal-boron separation, see Table II, however, the M -B distance is generally smaller in the present model than in the solids. For monovalent cations, it is systematically underestimated by more than 10%. For divalent cations, this difference is below 10% and for aluminum the equilibrium separation compares rather well to that observed in the crystalline phase.

The above analysis indicates that the monodentate orientation is energetically unfavorable for metal tetrahydroborates and tridentate arrangement will be the one most likely to occur in the solid structures. However, in the compounds considered here, the bidentate orientation is also observed in the crystalline phase. This suggests that effects beyond the scope of the present model are crucial for determining the solid-state structure. It becomes clear at this point that differences in covalent interaction, orbital overlap, and charge transfer between the metal atoms and the BH_4 groups do not explain the bidentate orientation that occurs in the solids.

D. Three-dimensional coordination of cations

The planar model presented in the previous section reveals a correlation between the radius of the metal cation and the metal- BH_4 separation. However, the coordination number for a given cation and the optimal orientation of the BH_4 groups with respect to the metal atom for that coordination cannot be calculated that way. Therefore, we now continue our analysis with an extended model that consists of three-dimensional (3D) structures relevant for the local geometry. This model provides the simplest way to discriminate between the different orientations of the BH_4 groups. The simplest three-dimensional model includes metal atoms tetrahedrally coordinated by tetrahydroborate groups. Such a model takes into account the attractive interaction between ions of opposite charge, the repulsive interaction between ions with the same charge state, and nonionic interactions such as orbital overlaps.

These calculations were performed using supercells with edges of at least 18 Å. For a set of metal-boron separations, the orientation of the hydrogen atoms was relaxed (each BH_4 group was allowed to freely reorient, keeping the boron positions fixed). We add extra electrons to the (neutral) system such that, accounting properly for the oxidation state of the metal ions, the formal charge on each BH_4 is $-1e$. To compensate for these, a uniform background charge was imposed on the system. We limit our analysis to divalent cations, hence the charge on the metal ions is $+2e$. In Fig. 2, the total energy of the system consisting of the divalent metals surrounded by four BH_4 groups as a function of metal-boron spacing is presented for bidentate, tridentate, and arbitrary BH_4 orientations.

For $\text{Ca}(\text{BH}_4)_2$, the equilibrium separation between tetrahydroborate groups and the metal is larger than ~ 2.6 Å. The analysis for this compound gives only qualitative aspects since the tetrahedral coordination cannot be compared directly to the real crystal structure since there each Ca cat-

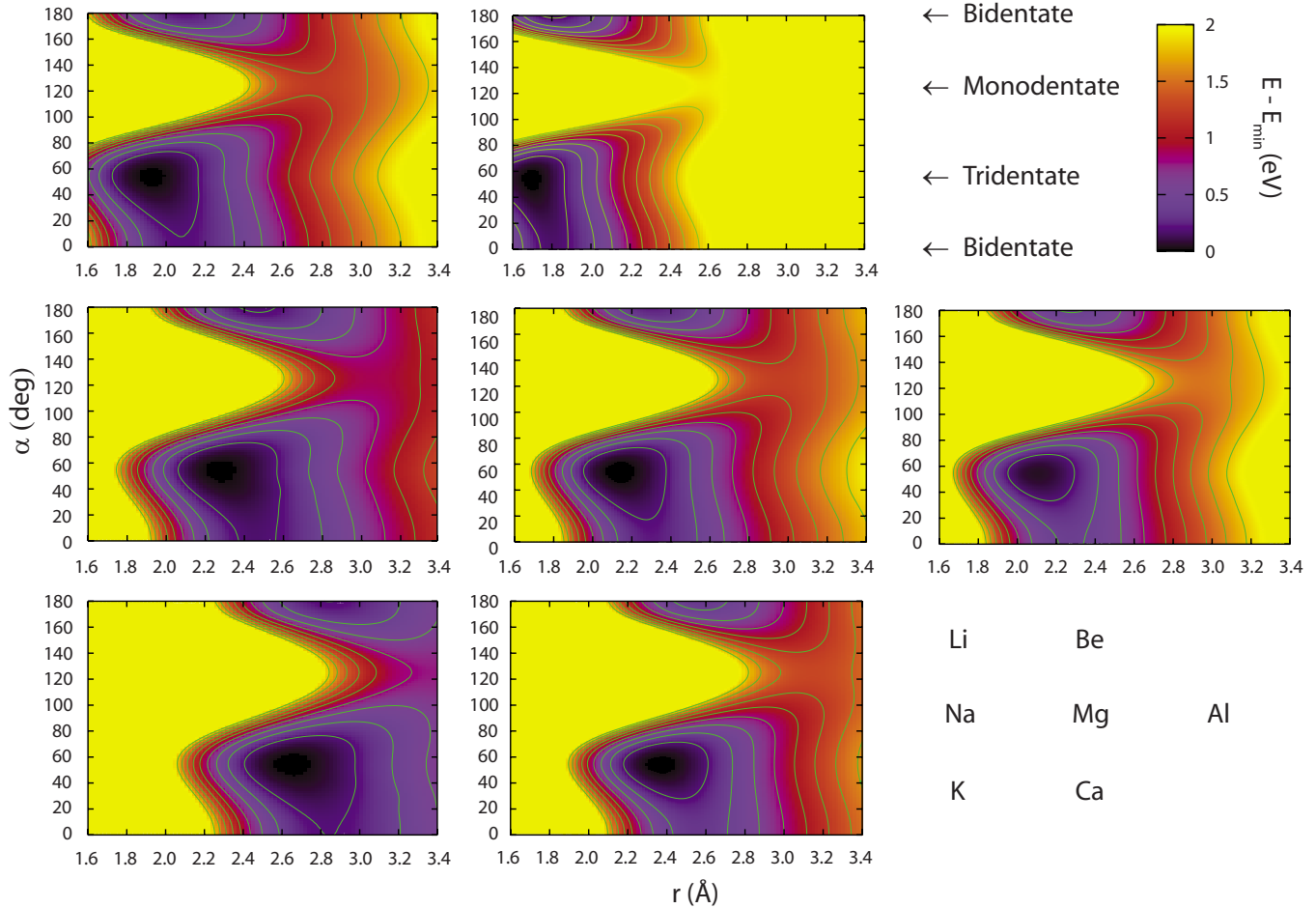


FIG. 1. (Color online) Potential energy surface for a BH_4 group interacting with a cation. All total energies are aligned to be zero at the minimal energy. The isolines are at 0.2 eV separation. The y axis denotes the rotation angle and the x axis the boron cation separation. The radial resolution of the underlying calculations is 0.1 Å and an angular resolution of 10° is applied. The plots are drawn applying a cubic spline to this data, the contours are also plotted using a cubic spline.

ion is surrounded by six BH_4 groups. The origin for this being the optimal coordination will be explained below. For the purpose of the present model we only point out that there is no preferential orientation of BH_4 group with respect to

TABLE II. Ion sizes and interatomic distances for the metal tetrahydroborates considered in this work. Under, R_S : the ionic radius according to Shannon (Ref. 59), $d(M\text{-B})$: the cation-boron distance as in the crystal structure of the solid, and under bidentate and tridentate: the minimum-energy distance for a single BH_4 group interacting with the specific cation in the respective orientation.

System	R_S	$d(M\text{-B})$	Bidentate	Tridentate
LiBH_4	0.59	2.50	2.1	1.9
NaBH_4	1.02	3.00	2.5	2.3
KBH_4	1.38	3.34	2.8	2.6
$\text{Be}(\text{BH}_4)_2$	0.16	1.89	1.8	1.7
$\text{Mg}(\text{BH}_4)_2$ ^a	0.57	2.40	2.3	2.1
$\text{Ca}(\text{BH}_4)_2$ ^b	1.00	2.90	2.6	2.4
$\text{Al}(\text{BH}_4)_3$	0.39	2.14	2.3	2.1

^aF222.

^b $P4_2/m$.

Ca, i.e., the bidentate and tridentate orientations are energetically equivalent, see Fig. 2.

For $\text{Mg}(\text{BH}_4)_2$, the equilibrium metal- BH_4 separation is ~ 2.4 Å, which compares well to the separation in the bulk crystal structure. This indicates that, besides the ionic attraction between Mg and BH_4 , the mutual repulsion between BH_4 groups plays a significant role in determining of the local cluster geometry. For this compound, there is a preference for the bidentate and even for distorted bidentate, orientation of the BH_4 around Mg.

For $\text{Be}(\text{BH}_4)_2$, which contains the smallest of all cations considered here, the tridentate orientation of the BH_4 is strongly unfavorable and a strong preference for the bidentate orientation is observed, see Fig. 2. Moreover, for this compound a threefold coordination of the Be is preferred over a fourfold coordination. This coordination number change is accompanied by an energy gain of more than 1 eV due to the detachment of a $(\text{BH}_4)^-$ group, see lower left corner of Fig. 2. Such preference properly reveals a threefold coordination of Be in the crystalline phase and a bidentate orientation of BH_4 groups.

The separation between the metal atoms and the BH_4 group in this model is comparable to that in the real bulk crystal structures, see Table I, even though the charge trans-

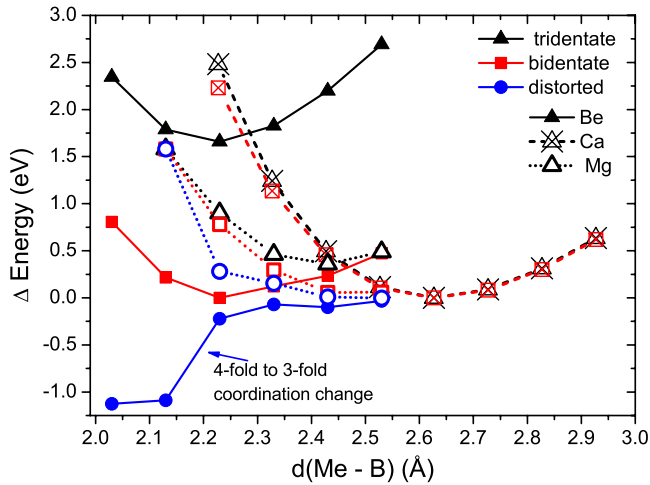


FIG. 2. (Color online) The total energy of the system for different BH_4 orientations as a function of cation-anion separation for tetrahedrally coordinated divalent cations Be, Mg, and Ca. Solid symbols are for Be, open ones for Mg, and crossed symbols are for Ca. Orientation of BH_4 anions is tridentate—triangles (black), bidentate—squares (red), and arbitrary (including distortion of tetrahedra around metal cation) that minimize total energy of the system—circles (blue).

fer between the atoms is different; for the present 3D model we assumed formal charges on the atoms of $+2e$ on the metals and $-1e$ on the BH_4 groups. In reality, these charges are smaller, see Table I, and the dielectric properties of these kinds of crystals are significantly different from those of the vacuum.⁶⁰

The important phenomenon revealed by this 3D cluster model is that for a small separation between the metal and the BH_4 group the preferential orientation of the BH_4 group around central metal cation may change from tridentate to bidentate, which are the orientations most often observed in the crystal structures. The mutual repulsion between the anions is an additional feature in the 3D model with respect to the model presented in the previous section. Thus, one might relate changes in the BH_4 orientation to the electrostatic effects. In the following paragraphs we will propose a simple model that clarifies, both qualitatively and quantitatively, the effect of this repulsion in details.

Orientation of BH_4

In order to understand orientation of BH_4 groups around the metal cation we propose now a simple model that focuses solely on the electrostatic repulsion between BH_4 groups. According to the charge distribution analysis presented in Table I, all hydrogen atoms carry a negative charge. We assume this point charge to be equal on every H atom. We consider each BH_4 group as a rigid body, i.e., neglect modification of their shape and B-H bond lengths. Each BH_4 cluster may rotate around the central boron atom and we describe this rotation by two angles. The angle α denotes rotation around the axis which is perpendicular to the metal-boron bond (see Fig. 3). The second rotation axis is parallel to the metal-boron bond and is described by the angle β . The BH_4

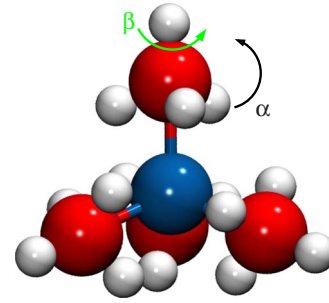


FIG. 3. (Color online) Schematic view of the rotation axes that are considered in the model for electrostatic interaction. BH_4 molecules are in tridentate configuration, the initial positions of the model (all angles are with respect to this orientation). Light gray (red) spheres are for boron, central gray (blue) one for metal, and small white ones are for hydrogen.

molecules are separated from the cation by a distance l that is expressed as the ratio between the metal-boron and B-H bond lengths. This ratio is small for the $\text{Be}(\text{BH}_4)_2$ system and increases for the other elements. In fact, the B-H bond is ~ 1.2 Å for all compounds and the metal-boron spacing ranges from ~ 1.90 to ~ 3.4 Å. We take for a small spacing the ratio $l = \frac{d_{M-B}}{d_{B-H}}$ to be 1.2 and 1.9 for larger spacing. The dielectric properties of the system are homogeneous. For our choice of the initial conditions ($\alpha = \beta = 0^\circ$), the orientation of BH_4 is tridentate for angles $\alpha = 0^\circ$ and $250^\circ 13'$. For $\alpha = 125^\circ 06'$ and $305^\circ 06'$, BH_4 groups are in bidentate orientation and for $\alpha = 70^\circ 13'$ and 180° in monodentate orientation. For the tridentate orientation, rotation around axis β reveals threefold symmetry.

The electrostatic potential energy of the system can be expressed as $V = \sum_{i,j} \frac{e^2}{r_{i,j}}$, where i, j runs over all hydrogen atoms from different BH_4 groups with $r_{i,j}$ the distance between them. The interaction between H atoms from the same BH_4 unit can be neglected, as the BH_4 group is considered to be a rigid body and this interaction will introduce an additive constant only. The orientation of each of the four BH_4 groups is the same with respect to the initial position, i.e., they are symmetrically equivalent. All BH_4 rotate simultaneously by the same angle. Their orientation can be expressed by two rotation matrixes $r = \mathbf{R}_\beta \cdot \mathbf{R}_\alpha \cdot \mathbf{r}_0$, where \mathbf{R}_β is the rotation β and \mathbf{R}_α is the rotation α . It is important to note that a rotation is first performed by the angle α and then by the angle β . The angle α defines the orientation of the BH_4 's with respect to the metal, i.e., monodentate and bidentate. The angle β subsequently changes the orientation of the BH_4 's with respect to each other, at that specific BH_4 -metal orientation, i.e., the angle β does not change the metal-hydrogen distances.

The potential-energy surfaces of the four BH_4 groups in tetrahedral coordination around a central metal cation are presented in Fig. 4(a) for small separation ($l = 1.2$) and in Fig. 4(b) for large separation ($l = 1.9$). For the BH_4 groups being close to the metal cation the potential is complex. In this case, numerous local minima indicate that energetic preference for tridentate ($\alpha \sim 0^\circ$ and $\sim 250^\circ$) orientations is accompanied by energetically competitive bidentate ($\alpha \sim 125^\circ$ and $\sim 305^\circ$) arrangement. Most of the energy minima are rather

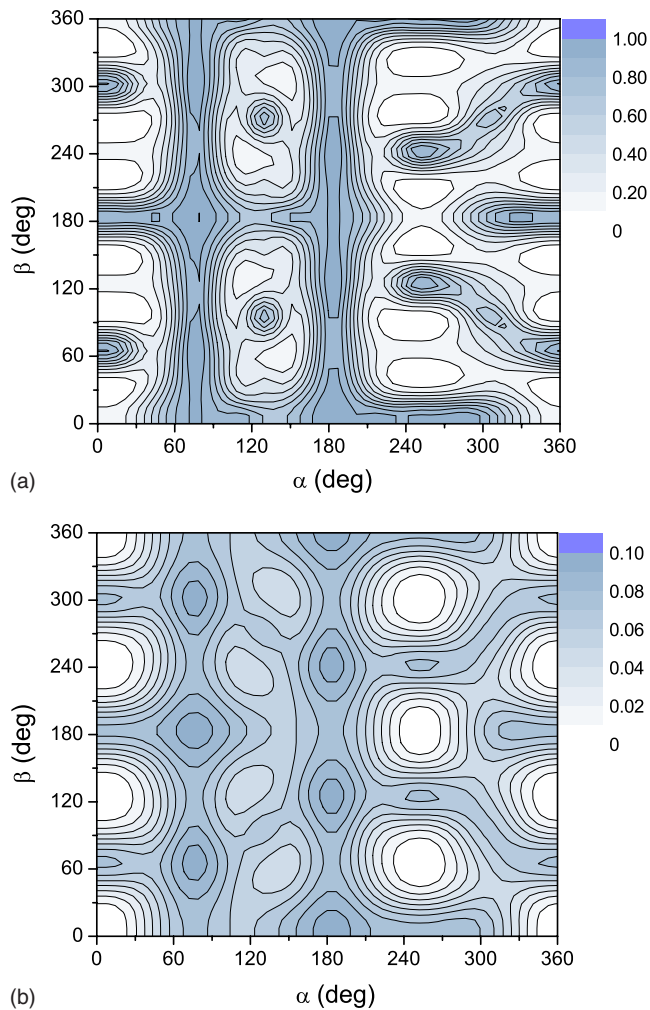


FIG. 4. (Color online) The potential-energy surface for BH_4 orientation tetrahedrally arranged around metal cation. (a) for short metal boron distance and (b) for large distance. The energy scale is normalized to one in (a) and the same normalization constant is used in (b) for easier comparison. The meaning of angles α and β is explained in the text and in Fig. 3. Monodentate orientation is for angles $\alpha=70^\circ 13'$ and 180° ; bidentate for $\alpha=125^\circ 06'$ and $305^\circ 06'$; and tridentate for $\alpha=0^\circ$ and $250^\circ 13'$.

smearred and connected such that distinct orientations are energetically equivalent. However, the local minima for bidentate orientation (at $\alpha \sim 125^\circ$) are separated by large energy barriers.

For large l , the tridentate orientation is the most stable arrangement of the BH_4 groups around the metal cation, Fig. 4(b), and two well-defined equivalent arrangements exist for $\alpha \sim 0^\circ$ and $\alpha \sim 250^\circ$. For larger separation, the electrostatic contribution to the total energy of the system is an order of magnitude smaller than for the situation shown in Fig. 4(a). Thus, our simple model indicates that, when considering electrostatic repulsion between multiple BH_4 's tetrahedrally arranged around metal cation, the bidentate and tridentate orientations become energetically competitive; this is in contrast to the one-dimensional model where the tridentate orientations were distinct and separated energy minima.

From simplified models presented above the following conclusions can be drawn: (i) the equilibrium distance be-

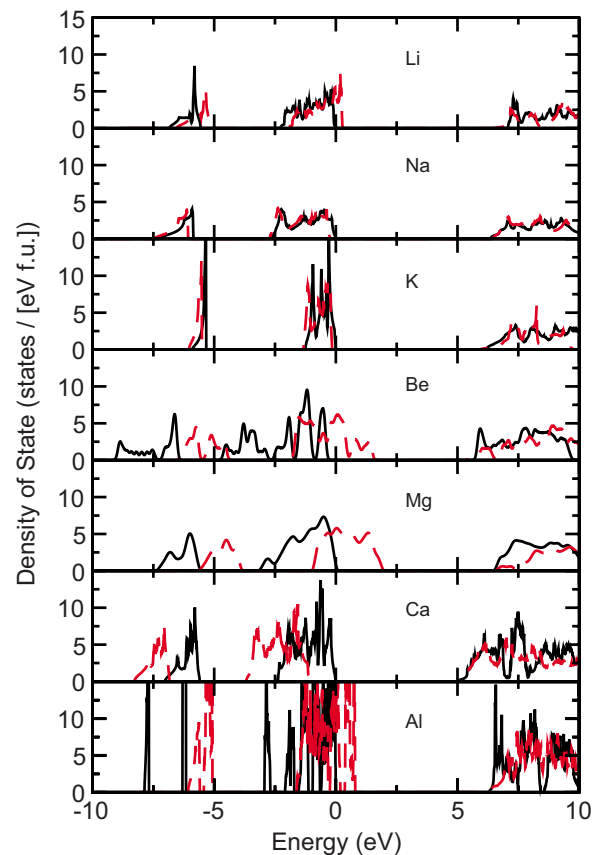


FIG. 5. (Color online) Total density of states (states/[formula unit eV]) for all materials discussed. The solid lines show the DOS of the complete materials, zero of energy is placed at the top of the valence band and the dashed line shows the DOS of the systems where the cations have been replaced by a homogeneous background. For the sake of the argument, see text, these are aligned to the DOSs of the original system such that the bottoms of the conduction bands are at the same energy.

tween BH_4 and metal as well as coordination number for the metal cation is determined by the type of metal (Fig. 2); (ii) the orientation of BH_4 group with respect to central metal depends on the separation between metal and boron (Figs. 1 and 4); (iii) the energy scale of ~ 1 eV related to reorientation of BH_4 group indicates that the local interactions “locks” bidentate or tridentate orientation of borohydride group, even in the crystalline phase (Fig. 1).

E. Electronic structure in the solids

Next, we return to the solids and discuss their interatomic bonding in relation to their electronic structure. We do this by comparing the total densities of states (DOSs) to those of the systems where the cations are replaced by a homogeneous background charge (HBG). Comparison of changes in the DOSs caused by such replacement provides information on the influence of the cations and, hence, on their binding to the anions. For all calculations here, the positions of the boron and hydrogen atoms are kept fixed. The DOSs of the materials studied in this paper are presented in Fig. 5. Except

for that of $\text{Al}(\text{BH}_4)_3$, they have been treated before in various publications.^{28,56,61–63}

In the majority of cases, replacing the cations by an HBG does not change the DOSs significantly. From this we can conclude that both the valence and the conduction bands are primarily of anionic character. An important ingredient for the explanation of the features discussed below is the difference in localization between the conduction and valence states. The valence states are more localized than the conduction states and, hence, will be more affected by replacement of the cations by an HBG. To show the effects of the replacements in a more transparent way, the DOSs of the systems with HBG are aligned in such a way to the DOSs of the original systems that the bottoms of the conduction states are located at the same energy.

In the Li-Na-K series, no significant changes in the density of states upon replacing the metal ions by an HBG can be observed. This implies that the DOSs are predominantly of anion nature, both in the valence region and in the conduction region, and the interaction is almost purely electrostatic. The one-to-one ratio between the ions causes the cations to be spread already rather homogeneously. In the case of Li, the band gap is slightly larger when the cations are present. Due to the small size of the Li cations they are close to the BH_4 groups and, hence, produce a slightly stronger electrostatic potential on the anion valence states when present than in the case when they are replaced by an HBG. The valence states on the BH_4 clusters are more localized than the conduction states, see Fig. 5. The replacement of the cations by the HBG will, therefore, leave the conduction states at the same energy but will increase the energy of the valence states, decreasing the band gap. Such effect has been shown previously also for the tetrahydroaluminates.⁶⁰

In the cases of Be, Mg, and Al, the band gap contracts in a similar way as in the case of Li. Again, the cations are small and relatively close to the tetrahydroborate groups. Replacing them by an HBG decreases the strength of the electrostatic potential acting on the hydrogen atoms, which results in the contraction of the band gap.

For Ca the band gap strongly increases. In this case, the cation has such a distance to the BH_4 groups that the electrostatic potential at the hydrogen atoms is increased in strength by replacing the cations by an HBG. The same effect occurs in the case of Na and K. However, since the charge of the cation is only half of that of Ca, the effect is much less pronounced for Na and K.

Only in the Be and Al case the valence region of the DOS changes when the metal ion is replaced by a homogeneous background charge. For both compounds there are “bonding states” (i.e., overlap of the atomic orbitals at the lower ends of the valence band) that are only present when the ions with their atomic orbitals are present. As was noted in the discussion in the previous sections, in these materials the atomic packing enforces threefold coordination, causing intrinsically different surroundings to occur for the hydrogen atoms. When the cations are replaced by an HBG this difference is mostly lifted and these bonding states disappear. The present analysis together with Bader valence charge analysis points out that the compounds considered here are strongly ionic systems, where the charge transfer is responsible for the crystal cohesion.

F. A general rule for coordination

The effective packing of atoms in the crystal structure depends primarily on factors such as: interaction between atoms and sizes of the atoms. We have shown that ions in metal tetrahydroborates are interacting mainly via electrostatic forces and that variation in the structural details between systems is then caused by different sizes of the metal cations and orientation of the tetrahydroborate group. Indeed, neither does a BH_4^- group significantly change in geometry nor do the B-H bond lengths for different cations. Therefore, it can be approximated by a spherical atom of the radius r_{BH} . The details of the mutual orientation of neighboring groups will be discussed below.

Being almost purely ionic systems, metal tetrahydroborates fall into a category of compounds already classified by L. Pauling with simple rules for atomic packing.⁶⁴ The coordination of the metal in tetrahydroborate depends on the ratio between the metal ionic radius (r_M) at appropriate charge state and the dimension of the BH_4^- group (r_{BH}). To apply the Pauling rules to the compounds studied here, one has to know the ionic radius of the BH_4^- group. Since this is not a well-defined quantity due to the tetrahedral shape of this molecule and its anionic character, we use reasonable ranges of these radii to classify compounds as presented in Fig. 6. The different solid lines for each compound stand for different metal ionic radii proposed by Shannon.⁵⁹ The dashed lines represent a fixed metal-boron distance, the one occurring in the solid. The rectangles mark regions where these two types of lines intersect. The ionic radius for each metal is taken for the appropriate oxidation state and two border lines span the region of radii: the lower line (lower right corner) is for a lower coordination (for example, threefold for Be) while the upper line (upper left corner) is for higher coordination (tetrahedral for Be).

For Be, Ca, and Na the Pauling rules ascribe correctly the atomic coordination for a broad range of anionic radii between 1.5 and 2.0 Å [this range is reasonable in view of experimentally suggested 1.9 Å (Ref. 65)] as threefold for Be and sixfold for Ca and Na. On the other hand, both LiBH_4 and $\text{Mg}(\text{BH}_4)_2$ have reasonable ionic radii ratio spans over tetrahedral and octahedral regions. This is reflected in known complications related to both structures: for LiBH_4 , there is still some inconsistency between experimental and theoretical studies in understanding of the phase transition and symmetry of the high-temperature phase.^{20,21} The experimental structure of $\text{Mg}(\text{BH}_4)_2$ is rather complicated with large unit cell^{22,23} while theoretical models reveal relatively simple structures.^{26–28} The $\text{Al}(\text{BH}_4)_3$ is not a purely ionic system and the Al coordination is related to the molecular structure of this compound.

Based on the above analysis, the Pauling rules applied to metal tetrahydroborates can be summarized as follows:

(I) *A coordinated polyhedron of anions is formed about each cation, the cation-anion distance being determined by the radius sum and the coordination number of the cation by the radius ratio.*⁶⁴ This rule determines the coordination number of the cation and the mutual arrangement of cations affects BH_4^- orientation.

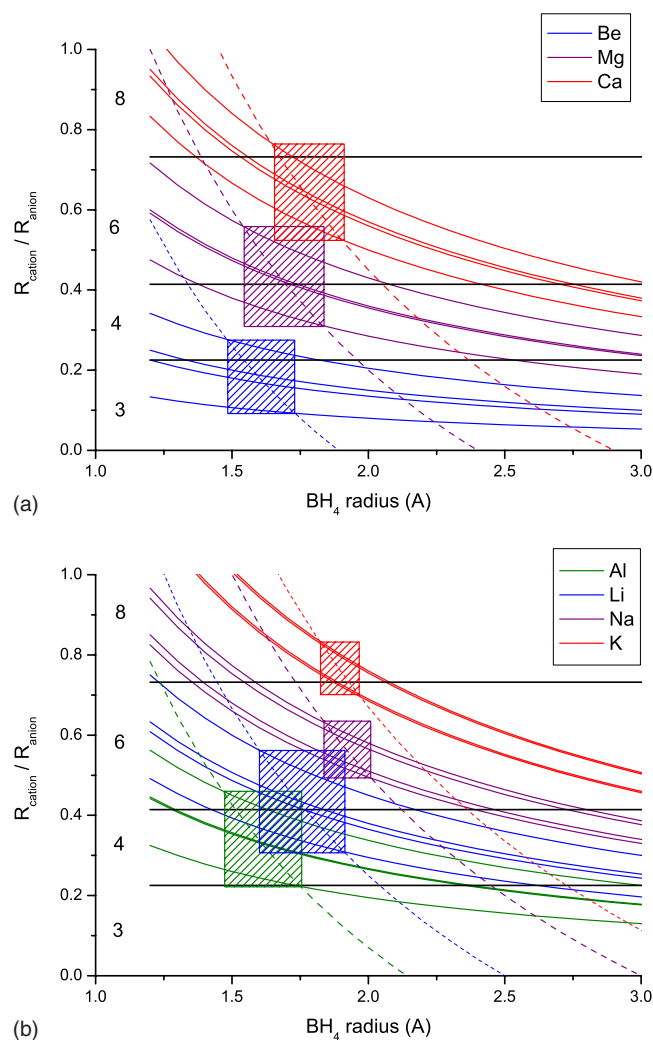


FIG. 6. (Color online) The ratio of the metal ionic radius as a function of BH_4 radius. (a) Top—divalent metal cations and (b) bottom—monovalent metals and Al. The multiple lines cover the variety of ionic and atomic radii as given in Ref. 59. The squares denote the most reasonable range of BH_4 radius. The horizontal lines distinguish different coordinations according to Pauling classification, see Table III.

(II) *In a stable coordination structure the electric charge of each anion tends to compensate the strength of the electrostatic valence bonds reaching to it from the cations at the centers of the polyhedra of which it forms a corner; that is, for each anion.*⁶⁴ This has to be fulfilled for all stable compounds.

(III) *The presence of shared edges, and particularly of shared faces, in a coordinated structure decreases its stability; this effect is large for cations with large valence and small coordination number and is especially large in case the radius ratio approaches the lower limit of stability of the polyhedron.*⁶⁴ This rule has a consequence for the preferential orientation of BH_4 groups. Both for systems sharing polyhedron edges or facets, only bidentate BH_4 orientation offers the opportunity to avoid highly unstable monodentate orientation. Especially for small cations, highly complex potential-energy surfaces can be encountered, due to orienta-

tion of BH_4 . This rule is also more important for cations with larger valency and smaller cation coordination number. For cations with valencies larger than three application of the Pauling rules is limited for metal tetrahydroborates, as these compounds (containing transition metals) makes a significant contribution to the covalent bonding between metal and BH_4 group and these bonds are directional.

Coordination	NN	$x=r_M/r_{\text{BH}}$	System
Trigonal	3	0.155–0.225	Be(3), Al(3/4)
Tetrahedral	4	0.225–0.414	Li(4/6), Mg(4/6)
Octahedral	6	0.414–0.732	Na(6), K(6/8), Ca(6)
Cubic	8	0.732–1.0	
Cubic/hexagonal	12	1.0	

(IV) *In a crystal containing different cations, those of high valency and small coordination number tend not to share polyhedron elements with each other.*⁶⁴ This rule indicates that complex metal tetrahydroborates containing different metal cations with different valency shall segregate, as long as they can be considered as ionic structures.

(V) *The number of essentially different kinds of constituents in a crystal tends to be small.*⁶⁴ This suggests that the stability of metal tetrahydroborates decreases when different metal cations constitute the compound as long as the system can be considered as ionic. The latter two rules state that formation of tetrahydroborates containing mixed metal cations might be hampered, especially for metals with low oxidation state.

In Table III, the range of ionic radii ratio for possible coordination is presented and the compounds studied here are assigned to the appropriate groups. $\text{Al}(\text{BH}_4)_3$ which forms the molecular crystals consisting of stoichiometric units has a threefold coordination and these entities are bonded via van der Waals forces in the crystalline phase. Also, the attractive interaction between aluminum and BH_4 groups is not purely ionic, as it includes bonding states below the Fermi level.⁶⁶ This type of structure cannot be simply classified by Pauling rules while according to Pauling classification the molecular nature of the crystal can be predicted correctly.

For $\text{Mg}(\text{BH}_4)_2$, the Pauling rules together with experimental and theoretical evidence provide coordination that is on the border line between tetrahedral and octahedral one. A dense packing of tetrahedra, however, poses an unsolvable problem since the dihedral angle ($\sim 70.53^\circ$) is not a submultiple of 360° .⁶⁷ Thus, the Euclidean three-dimensional space cannot be filled with tetrahedral objects without holes or empty spaces. This is well known for metal oxides with tetrahedral coordination which display a large variety of phases. For example in silica, SiO_2 (Refs. 68 and 69) [or germania, GeO_2 (Ref. 70)] all crystalline phases, except for

Sc (III) O	Ti (III) O/T (IV) T	V (II) O (III) O/T (IV) T	Cr (II) O (III) T	Mn (II) T/O (IV) T	Fe (II) T/O (III) T	Co (II) T (III) T (IV) T	Ni (II) T	Cu (I) T (II) T	Zn (II) O/T
Y (III) O	Zr (IV) T	Nb (III) O (IV) O	Mo (III) O (IV) O/T (VI) T	Element (oxidation state) coordination					Cd (II) O

FIG. 7. (Color online) The coordination of the metal cation in selected metal tetrahydroborates with high weight content of hydrogen. The Roman digits are for the oxidation states, T stands of tetrahedral and O stands for octahedral coordination. T/O (O/T) is for elements for which no clear distinction local coordination number can be established. The shaded (green) cells are for metal tetrahydroborates with resolved crystal structure that possess cation coordination as predicted by our model.

high pressure and fibrous ones, consist of SiO_4 (GeO_4) tetrahedra linked together by shared vertices of different arrangement. More than six phases of these compounds are known. From the atomic packing point of view, a similar situation is observed for magnesium tetrahydroborate. Here, an additional degree of freedom comes from the orientation of BH_4 group. A variety of phases with nearly degenerate formation energies were reported by theoretical calculations. In particular, for the lowest-energy structure $F222$ (Ref. 27) BH_4 groups are separated by ~ 2.4 Å from Mg and they are slanted by $\sim 10^\circ$ from the ideal bidentate orientation. In another calculated low energy structure $I\bar{4}m2$,²⁶ magnesium boron separation remains similar, however orientation of BH_4 groups is bidentate.

In the experimental α phase of this compound with $P6_1$ symmetry,^{23,24} the orientation of BH_4 groups ranges from ideal bidentate to slanted by more than 10° , with the coordination tetrahedron being distorted. Such an effect leads to orientational frustration in the BH_4 sublattice, which is close in energy to the optimal local geometry due to the complex potential-energy surface for BH_4 alignment as shown in Fig. 4(a). The local distortions in the experimental structure enable the system to obtain the higher density.

Both calculated low-energy structures possess a density that is considerably lower than reported experimentally (~ 0.55 g cm^{-3} vs ~ 0.8 g cm^{-3}).²⁷ Due to the nature of the theoretical models they do not contain entropy contributions related to the large-scale disorder of tetrahedral structural building blocks. Additionally DFT lacks the presence of weak interactions such as van der Waals. Since, these interactions will have a larger contribution to the structures with a higher density, the high-density structures will appear as a less stable than those with a low density in DFT. In a case like $\text{Mg}(\text{BH}_4)_2$, where due to the complex potential-energy surface for BH_4 alignment the total energies of various structures are very close, these two effects can interchange the relative stability of high- and low-density phases in DFT compared to reality. The final effect being that the high-density structures are less stable in DFT but more stable when the interactions missing in DFT are present.

III. COORDINATION IN METAL BOROHYDRIDES

Based on the model proposed in this paper, one can predict the atomic coordination for metal tetrahydroborates with

a high weight content of hydrogen, as presented in Fig. 7. This coordination is related to the crystalline structure and the nature of compound. For example, both $\text{Sc}(\text{BH}_4)_3$ and $\text{Y}(\text{BH}_4)_3$ will possess an octahedral coordination, and they will not form molecular crystals, such as $\text{Al}(\text{BH}_4)_3$, unless there is a strong covalent contribution to the bonding between metal and BH_4 . Indeed, a reported phase of $\text{Y}(\text{BH}_4)_3$ has $Pa\bar{3}$ symmetry with octahedral coordination.⁷¹

For the majority of light transition metals the cations will possess a tetrahedral (or border line between octahedral and tetrahedral) coordination, even though a variety of oxidation states are possible for these elements. This means that tetrahydroborate of Zr should be formed from stoichiometric molecules $\text{Zr}(\text{BH}_4)_4$ and that ionic crystalline structures can be found for those of Cu, Mn, Fe, Co, Ni, or Zn. The preference for tetrahedral coordination (for divalent metals) suggests that their structure will not be simple, similarly as for $\text{Mg}(\text{BH}_4)_2$. Recently reported structure for $\text{Mn}(\text{BH}_4)_2$ seems to confirm our predictions.⁷² Figure 7 could serve as a guideline for characterization and design of new compounds. One has to keep in mind, however, that especially for small cations (Ni, Cu) hybridization of the metal d orbitals and valence states of BH_4 groups may lead to preference for solid phases consisting of molecular metal- BH_4 structures.

IV. CONCLUSIONS

In this paper, we have revealed the relation between bonding and the structure of metal tetrahydroborates. From Bader charge analysis and a detailed analysis of the DOSs of the complex hydrides we have shown that the systems are strongly ionic for monovalent and divalent cations.

Using DFT, we have shown that the interaction between a single BH_4 group and a cation favors a tridentate orientation. However, when the interaction of multiple BH_4 groups is taken into account the bidentate orientation becomes almost degenerate in energy with the tridentate orientation. By constructing an analytic model of the electrostatic interactions we have shown that the BH_4 orientation can be understood from electrostatic repulsion between the H^- .

The ionic radius of the cation (which determines the cation/anion radii ratio) finally establishes the global geometry according to the Pauling rules for ionic crystals. In the alkali tetrahydroborates, octahedral coordination is preferred for NaBH_4 and KBH_4 and tetrahedral for LiBH_4 . As the

separation between cation and anion is relatively large for these compounds, the bidentate orientation of BH_4 groups results as the optimal one for shared vertices and edges of the coordination polyhedra.

For divalent metals, the ionic radii span a larger range. In $\text{Be}(\text{BH}_4)_2$, due to the size of the Be^{2+} only a threefold coordination by BH_4 groups is predicted by the Pauling rules, as observed in the crystal structure.⁵⁶

For magnesium borohydride, the Pauling rules predict a tetrahedral or octahedral coordination. In known structures of this compound, four BH_4 groups surround each magnesium atom. However, due to the close proximity of these anions their mutual electrostatic repulsion enforces a complicated potential-energy landscape that is related to the local BH_4 orientation (see Fig. 4). Additional complications arise from the impossibility of complete space filling by tetrahedral objects. These factors result in an almost degenerate global energy landscape for the crystal structure forming a 3D network with large cavities. This produces the variety of equivalent crystalline symmetries that are degenerate in energy, similarly to oxides such as silica. Theoretically predicted lowest-energy structures of $\text{Mg}(\text{BH}_4)_2$ possess low

density (low filling ratio of the space) because theoretical models account for strong local interactions while the experimental structures are denser and the free energy large-scale entropic contribution due to disorder of building blocks together with a weak dispersive interaction prevents them achieving predicted symmetries and simpler primitive unit cells.

The large dimension of calcium ions provides octahedral coordination with bidentate and tridentate orientations. For Al, the Pauling rules predict a tetrahedral orientation, however the stoichiometric molecular complex $\text{Al}(\text{BH}_4)_3$ is formed and no further network or chain can be formed. A weak van der Waals-type interaction binds the larger $\text{Al}(\text{BH}_4)_3$ complexes together into a molecular crystal.

ACKNOWLEDGMENTS

Financial support by the Netherlands Organization for Scientific Research (NWO) and cpu time allocation at CSCS Supercomputer Centre, Manno and on the OPUS^{LB} Cluster at the Karlsruhe Institute of Technology (KIT) Steinbuch Centre for Computing (SCC) are gratefully acknowledged.

*zbigniew.lodziana@ifj.edu.pl

¹G. Silbiger and S. H. Bauer, *J. Am. Chem. Soc.* **68**, 312 (1946).

²A. M. Soldate, *J. Am. Chem. Soc.* **69**, 987 (1947).

³P. M. Harris and E. P. Meibohm, *J. Am. Chem. Soc.* **69**, 1231 (1947).

⁴R. M. Rulon and L. S. Mason, *J. Am. Chem. Soc.* **73**, 5491 (1951).

⁵A. J. Stosick, *Acta Crystallogr.* **5**, 151 (1952).

⁶H. I. Schlesinger and H. C. Brown, *J. Am. Chem. Soc.* **75**, 219 (1953).

⁷S. W. Chaikin, *Anal. Chem.* **25**, 831 (1953).

⁸S. C. Abrahams and J. Kalnajs, *J. Chem. Phys.* **22**, 434 (1954).

⁹L. V. Titiv, *Dokl. Akad. Nauk SSSR* **154**, 654 (1964).

¹⁰B. D. James, R. K. Nanda, and M. G. H. Wallbridge, *J. Chem. Soc. A* (1966) 182.

¹¹B. D. James and M. G. Wallbridge, *J. Inorg. Nucl. Chem.* **28**, 2456 (1966).

¹²E. B. Lobkovskii, S. E. Kravchenko, and K. N. Semenenko, *J. Struct. Chem.* **18**, 312 (1977).

¹³V. I. Mikheeva, N. N. Maltseva, and N. S. Kedrova, *Zh. Neorg. Khim.* **24**, 408 (1979).

¹⁴J. S. Hummelshøj, D. D. Landis, J. Voss, T. Jiang, A. Tekin, N. Bork, M. Duřak, J. J. Mortensen, L. Adamska, J. Andersin, J. D. Baran, G. D. Barmparis, F. Bell, A. L. Bezanilla, J. Bjork, M. E. Björketun, F. Bleken, F. Buchter, M. Bürkle, P. D. Burton, B. B. Buus, A. Calborean, F. Calle-Vallejo, S. Casolo, B. D. Chandler, D. H. Chi, I. Czekaj, S. Datta, A. Dartye, A. DeLaRiva, V. Despoja, S. Dobrin, M. Engelund, L. Ferrighi, P. Frondelius, Q. Fu, A. Fuentes, J. Fürst, A. García-Fuente, J. Gavnholt, R. Goeke, S. Gudmundsdóttir, K. D. Hammond, H. A. Hansen, D. Hibbitts, E. Hobi, Jr., J. G. Howalt, S. L. Hruby, A. Huth, L. Isaeva, J. Jelic, I. J. T. Jensen, K. A. Kacprzak, A. Kelkkanen, D. Kelsey, D. S. Kesankurthi, J. Kleis, P. J. Klüpfel, I. Konstanti-

nov, R. Korytar, P. Koskinen, C. Krishna, E. Kunkes, A. H. Larsen, J. M. G. Lastra, H. Lin, O. Lopez-Acevedo, M. Mantega, J. I. Martínez, I. N. Mesa, D. J. Mowbray, J. S. G. Mýrdal, Y. Natanzon, A. Nistor, T. Olsen, H. Park, L. S. Pedroza, V. Petzold, C. Plaisance, J. A. Rasmussen, H. Ren, M. Rizzi, A. S. Ronco, C. Rostgaard, S. Saadi, L. A. Salguero, E. J. G. Santos, A. L. Schoenhalz, J. Shen, M. Smedemand, O. J. Stausholm-Møller, M. Stibius, M. Strange, H. B. Su, B. Temel, A. Tofte-lund, V. Tripkovic, M. Vanin, V. Viswanathan, A. Vojvodic, S. Wang, J. Wellendorff, K. S. Thygesen, J. Rossmel, T. Bligaard, K. W. Jacobsen, J. K. Nørskov, and T. Vegge, *J. Chem. Phys.* **131**, 014101 (2009).

¹⁵A. Züttel, A. Borgschulte, and S. Orimo, *Scr. Mater.* **56**, 823 (2007).

¹⁶M. Born, *Verh. Dtsch. Phys. Ges.* **21**, 679 (1919).

¹⁷M. J. van Setten, G. A. de Wijs, and G. Brocks, *J. Phys. Chem. C* **111**, 9592 (2007).

¹⁸G. Renaudin, S. Gomes, H. Hagemann, L. Keller, and K. Yvon, *J. Alloys Compd.* **375**, 98 (2004).

¹⁹P. Vajeeston, P. Ravindran, A. Kjekshus, and H. Fjellvag, *J. Alloys Compd.* **387**, 97 (2005).

²⁰Z. Łodziana and T. Vegge, *Phys. Rev. Lett.* **93**, 145501 (2004).

²¹Y. Filinchuk, D. Chernyshov, and R. Černý, *J. Phys. Chem. C* **112**, 10579 (2008).

²²J. Her, P. Stephens, Y. Gao, G. Soloveichik, J. Rijssenbeek, M. Andrus, and J. Zhao, *Acta Crystallogr., Sect. B: Struct. Sci.* **63**, 561 (2007).

²³R. Černý, Y. Filinchuk, H. Hagemann, and K. Yvon, *Angew. Chem., Int. Ed.* **46**, 5765 (2007).

²⁴Y. Filinchuk, R. Černý, and H. Hagemann, *Chem. Mater.* **21**, 925 (2009).

²⁵L. George, V. Drozd, S. K. Saxena, E. Gil Bardaji, and M. Fichtner, *J. Phys. Chem. C* **113**, 486 (2009).

- ²⁶V. Ozolins, E. H. Majzoub, and C. Wolverton, *Phys. Rev. Lett.* **100**, 135501 (2008).
- ²⁷J. Voss, J. S. Hummelshøj, Z. Łodziana, and T. Vegge, *J. Phys.: Condens. Matter* **21**, 012203 (2009).
- ²⁸M. J. van Setten, G. A. de Wijs, M. Fichtner, and G. Brocks, *Chem. Mater.* **20**, 4952 (2008).
- ²⁹B. Dai, D. S. Sholl, and J. K. Johnson, *J. Phys. Chem. C* **112**, 4391 (2008); X.-F. Zhou, Q.-R. Qian, J. Zhou, B. Xu, Y. Tian, and H.-T. Wang, *Phys. Rev. B* **79**, 212102 (2009).
- ³⁰P. Vajeeston, P. Ravindran, A. Kjekshus, and H. Fjellvåg, *Appl. Phys. Lett.* **89**, 071906 (2006).
- ³¹Y. Nakamori, K. Miwa, A. Ninomiya, H. W. Li, N. Ohba, S. I. Towata, A. Züttel, and S. I. Orimo, *Phys. Rev. B* **74**, 045126 (2006).
- ³²K. Miwa, M. Aoki, T. Noritake, N. Ohba, Y. Nakamori, S. I. Towata, A. Züttel, and S. I. Orimo, *Phys. Rev. B* **74**, 155122 (2006).
- ³³F. Buchter, Z. Łodziana, A. Remhof, O. Friedrichs, A. Borgschulte, Ph. Mauron, A. Züttel, D. Sheptyakov, G. Barkhordarian, R. Bormann, K. Chłopek, M. Fichtner, M. Sørby, M. Riktor, B. Hauback, and S. Orimo, *J. Phys. Chem. B* **112**, 8042 (2008).
- ³⁴M. D. Riktor, M. H. Sørby, K. Chłopek, M. Fichtner, F. Buchter, A. Züttel, and B. C. Hauback, *J. Mater. Chem.* **17**, 4939 (2007).
- ³⁵M. Fichtner, K. Chłopek, M. Longhini, and H. Hagemann, *J. Phys. Chem. C* **112**, 11575 (2008).
- ³⁶N. Hanada, W. Lohstroh, and M. Fichtner, *J. Phys. Chem. C* **112**, 131 (2008).
- ³⁷Y. Filinchuk, E. Roennebro, and D. Chandra, *Acta Mater.* **57**, 732 (2009).
- ³⁸E. H. Majzoub and E. Roennebro, *J. Phys. Chem. C* **113**, 3352 (2009).
- ³⁹Y.-S. Lee, Y. Kim, Y. W. Cho, D. Shapiro, C. Wolverton, and V. Ozolins, *Phys. Rev. B* **79**, 104107 (2009).
- ⁴⁰G. Barkhordarian, T. R. Jensen, S. Doppiu, U. Bösenberg, A. Borgschulte, R. Gremaud, Y. Cerenius, M. Dornheim, T. Klassen, and R. Bormann, *J. Phys. Chem. C* **112**, 2743 (2008).
- ⁴¹M. Aoki, K. Miwa, T. Noritake, N. Ohba, M. Matsumoto, H.-W. Li, Y. Nakamori, S. Towata, and S. Orimo, *Appl. Phys. A: Mater. Sci. Process.* **92**, 601 (2008).
- ⁴²J. Kim, S.-A. Jin, J. Shim, and Y. W. Cho, *J. Alloys Compd.* **461**, L20 (2008).
- ⁴³E. Rönnebro and E. H. Majzoub, *J. Phys. Chem. B* **111**, 12045 (2007).
- ⁴⁴M. D. Riktor, M. H. Sørby, K. Chłopek, M. Fichtner, and B. C. Hauback, *J. Mater. Chem.* **19**, 2754 (2009).
- ⁴⁵S. Aldridge, A. J. Blake, A. J. Downs, R. O. Gould, S. Parsons, and C. R. Pulham, *J. Chem. Soc. Dalton Trans.* (1997) 1007.
- ⁴⁶K. Miwa, N. Ohba, S. Towata, Y. Nakamori, A. Züttel, and S. Orimo, *J. Alloys Compd.* **446-447**, 310 (2007).
- ⁴⁷J. P. Perdew, J. A. Chevary, S. H. Vosko, K. A. Jackson, M. R. Pederson, D. J. Singh, and C. Fiolhais, *Phys. Rev. B* **46**, 6671 (1992).
- ⁴⁸G. Kresse and D. Joubert, *Phys. Rev. B* **59**, 1758 (1999).
- ⁴⁹P. E. Blöchl, *Phys. Rev. B* **50**, 17953 (1994).
- ⁵⁰G. Kresse and J. Furthmüller, *Phys. Rev. B* **54**, 11169 (1996).
- ⁵¹G. Kresse and J. Furthmüller, *Comput. Mater. Sci.* **6**, 15 (1996).
- ⁵²G. Kresse and J. Hafner, *Phys. Rev. B* **47**, 558 (1993).
- ⁵³J. Hafner, *J. Comput. Chem.* **29**, 2044 (2008).
- ⁵⁴S. G. Louie, S. Froyen, and M. L. Cohen, *Phys. Rev. B* **26**, 1738 (1982).
- ⁵⁵P. E. Blöchl, O. Jepsen, and O. K. Andersen, *Phys. Rev. B* **49**, 16223 (1994).
- ⁵⁶M. J. van Setten, G. A. de Wijs, and G. Brocks, *Phys. Rev. B* **77**, 165115 (2008).
- ⁵⁷G. Henkelman, A. Arnaldsson, and H. Jónsson, *Comput. Mater. Sci.* **36**, 354 (2006).
- ⁵⁸E. Sanville, S. D. Kenny, R. Smith, and G. Henkelman, *J. Comput. Chem.* **28**, 899 (2007).
- ⁵⁹R. D. Shannon, *Acta Crystallogr., Sect. A: Cryst. Phys., Diffraction, Theor. Gen. Crystallogr.* **32**, 751 (1976).
- ⁶⁰M. J. van Setten, V. A. Popa, G. A. de Wijs, and G. Brocks, *Phys. Rev. B* **75**, 035204 (2007).
- ⁶¹K. Miwa, N. Ohba, S. I. Towata, Y. Nakamori, and S. I. Orimo, *Phys. Rev. B* **69**, 245120 (2004).
- ⁶²T. J. Frankcombe, G. J. Kroes, and A. Züttel, *Chem. Phys. Lett.* **405**, 73 (2005).
- ⁶³Z. Łodziana, A. Züttel, and P. Zielinski, *J. Phys.: Condens. Matter* **20**, 465210 (2008).
- ⁶⁴L. Pauling, *J. Am. Chem. Soc.* **51**, 1010 (1929).
- ⁶⁵T. C. Pochapsky, A. P. Wang, and P. M. Stone, *J. Am. Chem. Soc.* **115**, 11084 (1993).
- ⁶⁶I. Demachy and F. Volatron, *Inorg. Chem.* **33**, 3965 (1994).
- ⁶⁷J. H. Conway and S. Torquato, *Proc. Natl. Acad. Sci. U.S.A.* **103**, 10612 (2006).
- ⁶⁸R. Martoňák, D. Donadio, A. R. Oganov, and M. Parrinello, *Nature Mater.* **5**, 623 (2006).
- ⁶⁹K. Taeck Park, K. Terakura, and Y. Matsui, *Nature (London)* **336**, 670 (1988).
- ⁷⁰Z. Łodziana, K. Parlinski, and J. Hafner, *Phys. Rev. B* **63**, 134106 (2001).
- ⁷¹T. Sato, K. Miwa, Y. Nakamori, K. Ohoyama, H.-W. Li, T. Noritake, M. Aoki, S. Towata, and S. Orimo, *Phys. Rev. B* **77**, 104114 (2008).
- ⁷²R. Černý, N. Penin, H. Hagemann, and Y. Filinchuk, *J. Phys. Chem. C* **113**, 9003 (2009).
- ⁷³See supplementary material at <http://link.aps.org/supplemental/10.1103/PhysRevB.81.024117> for the unit cells and atomic positions of the crystal structures of LiBH_4 , NaBH_4 , KBH_4 , $\text{Be}(\text{BH}_4)_2$, $\text{Mg}(\text{BH}_4)_2$, $\text{Ca}(\text{BH}_4)_2$, and $\text{Al}(\text{BH}_4)_3$ as used in this paper.